

Magnetic investigation of heavy metals contamination in urban topsoils around the East Lake, Wuhan, China

Tao Yang,^{1,2} Qingsheng Liu,¹ Lungsang Chan³ and Guodong Cao¹

¹Department of Geophysics, China University of Geosciences, Wuhan 430074, P. R. China. E-mail: lqs321@cug.edu.cn

²Sino-Hungarian Joint Laboratory of Environmental Science and Health, Wuhan/Budapest, China University of Geosciences, Wuhan 430074, P. R. China

³Department of Earth Sciences, The University of Hong Kong, Pokfulam Road, P. R. China

Accepted 2007 July 25. Received 2007 July 25; in original form 2007 January 7

SUMMARY

Magnetic measurements and heavy metal analyses were performed on 133 samples from the urban soils around the East Lake in Wuhan, China. Samples were collected from four areas with different environmental settings: a heavy industrial area well known for thermal power generation and steel works; villages located in the downwind area of the industrial area; a main road with heavy traffic and roads around the East Lake. Results show that concentrations of magnetic particle and heavy metals in urban topsoils are significantly elevated due to the input of coarser-grained magnetite from industrial (e.g. power generation and steel production) and other anthropogenic activities (e.g. vehicle emissions). Concentration-related magnetic parameters, for example, magnetic susceptibility, saturation isothermal remanent magnetization and anhysteretic remanent magnetization, significantly correlate with the concentration of heavy metals. Moreover, in terms of grain sizes, the magnetic particles of different origins can be efficiently discriminated at the studied region. Therefore, magnetic measurements provide a basis for discrimination and identification of different contamination sources, and can be used as an economic alternative to chemical analysis when mapping heavy metal contamination in urban soil around the East Lake region, Wuhan, China.

Key words: contamination, heavy metal, magnetic properties, the East Lake, urban soil, Wuhan.

1 INTRODUCTION

As a direct sink, urban soils suffer the deposition of various airborne particulates from anthropogenic activities. There are mainly four types of anthropogenic pollution for soils in the urban environment (1) ashes emitted from industrial production and fossil-fuel combustion, such as steel production and power generation; (2) particles from vehicles, such as exhaust particulates, brake lining dust, and erosion of bodyworks; (3) exotic materials, such as metallic fragments, slag, road surface and building materials and (4) fertilizers and pesticides transported from agricultural soils and sewage sludge. The first type is of the largest quantity, for example, in areas with a high concentration of industrial facilities, the annual amount of atmospherically deposited dust can reach several thousands of tons (Kapička *et al.* 2003). However, the most serious pollutants among these different types are heavy metals, such as Pb, Cd, Cu and Zn (DeKimpe & Morel 2000).

Soil magnetic measurements have been employed recently in estimating anthropogenic pollution in different countries (e.g. Dearing *et al.* 1996; Kapička *et al.* 1999, 2003; Petrovský *et al.* 2000b; Fialova *et al.* 2006; Lu & Bai 2006) on the basis of the assumption that the industrial processes, such as combustion of fossil fuel, produce fly ashes with significant portion of magnetic minerals

(Flanders 1994) that are transported through atmospheric pathways and deposited on the ground. These particles accumulate in top layers of soils, and their increased concentration can be easily detected using surface magnetic measurements (Lecoanet *et al.* 1999). Kapička *et al.* (1999) mapped the spatial distribution of pollutants and pollution load near a coal-burning power plant by measuring magnetic susceptibility. Yan *et al.* (2005) found that multidomain magnetite is a dominant magnetic mineral in the top 14 cm of the soil profile near a storage site for fly ash of a power plant in Zhejiang province, China.

Significant correlation between magnetic properties and heavy metal concentrations in soils were observed in numerous studies (e.g. Heller *et al.* 1998; Dearing *et al.* 2001; Jordanova *et al.* 2003; Lu & Bai 2006). Strzyszcz & Magiera (1998) reported a positive correlation between magnetic susceptibility and concentration of Zn, Pb and Cd in Polish topsoils. Schmidt *et al.* (2005) observed a strong correlation between magnetic susceptibility and heavy metal in a former industrial iron production and processing site near Bradford, England. Strong correlations have also been found between magnetic susceptibility and the concentration of Pb, Cd, Cu and Zn in urban soils in Hangzhou city, China (Lu & Bai 2006).

Despite much of the recent attention to heavy metals in the urban soils, magnetic measurements have been seen limited use in

examining the magnetic properties and their correlation with the concentration of heavy metals in urban soils in China (Yan *et al.* 2005; Wang & Qin 2006; Lu & Bai 2006; Shen *et al.* 2006). In the present work, we conduct detailed magnetic measurements and chemical analyses on the urban soils around the East Lake, Wuhan, China. The objectives of the study are threefold. First, we examine the magnetic properties of urban soils, and seek to understand their relationships with heavy metals concentration. Secondly, we would like to establish links between elevated concentrations of anthropogenic magnetic particles, heavy metals (e.g. Cu, Pb and Zn), and known sources of pollution. Lastly, we examine the feasibility of using these magnetic parameters as indicators of heavy metals pollution in the urban soils.

2 MATERIALS AND METHODS

2.1 Study area

The East Lake, the largest urban lake in China, is situated in the northeast of Wuhan, the largest city in central China and in the middle reaches of Yangtze River (Fig. 1). A number of roadway dykes (East Lake Road) have been constructed along the lake shore. Sediments in the near surface layers in this area are mainly Quaternary alluvial or diluvial deposit with low magnetic minerals content (the mass-specific susceptibility is about $20 \times 10^{-8} \text{ m}^3 \text{ kg}^{-1}$). The prevailing wind direction is northeast during entire year. Wuhan Iron and Steel Group (WISG), the third largest iron and steel consortium in China and Qingshan Thermal Power Plant (QTPP) with a

total installed capacity of 986 000 kW, lie to the northeast of the East Lake (Fig. 1). Qingwang Road lies east of the lake and is the main road connecting two major districts (Qingshan and Hongshan Districts) in Wuhan. In addition to buses and taxis, a great deal of trucks transporting building materials, raw materials, and produces for WISG, QTPP and other plants travel on this road. With the rapid industrialization and urbanization, environmental pollution around the East Lake has been constantly increasing during last two decades.

2.2 Sampling

The soil types in the study areas cover cumulic anthrosols and calcareous fluvisols that developed on recent river and lake sediments. Soil samples were collected from four areas (Fig. 1). The first area (WG) is close to WISG and QTPP; the second area (BYQ) consists of villages downwind from WISG and QTPP; the third area (ELR) is around the East Lake; and the fourth area (QWR) is along Qingwang Road. The sampling points were distributed over diverse locations. All 25 topsoil samples were collected from farmland in WG. In BYQ, 6 topsoil samples were collected from uncultivated land and 19 from farmland. In QWR, 5 topsoil samples were collected from uncultivated land and the rest 21 topsoil samples from farmland along the road. In ELR, 19 samples were collected from bare soil by roadside and 5 samples from the farmland nearby. At each sampling point, the upper 5 cm layer of the soil profile was collected from a square of $20 \times 20 \text{ cm}$ using a non-magnetic bamboo trowel. Subsoil samples were collected from depths of 20 to

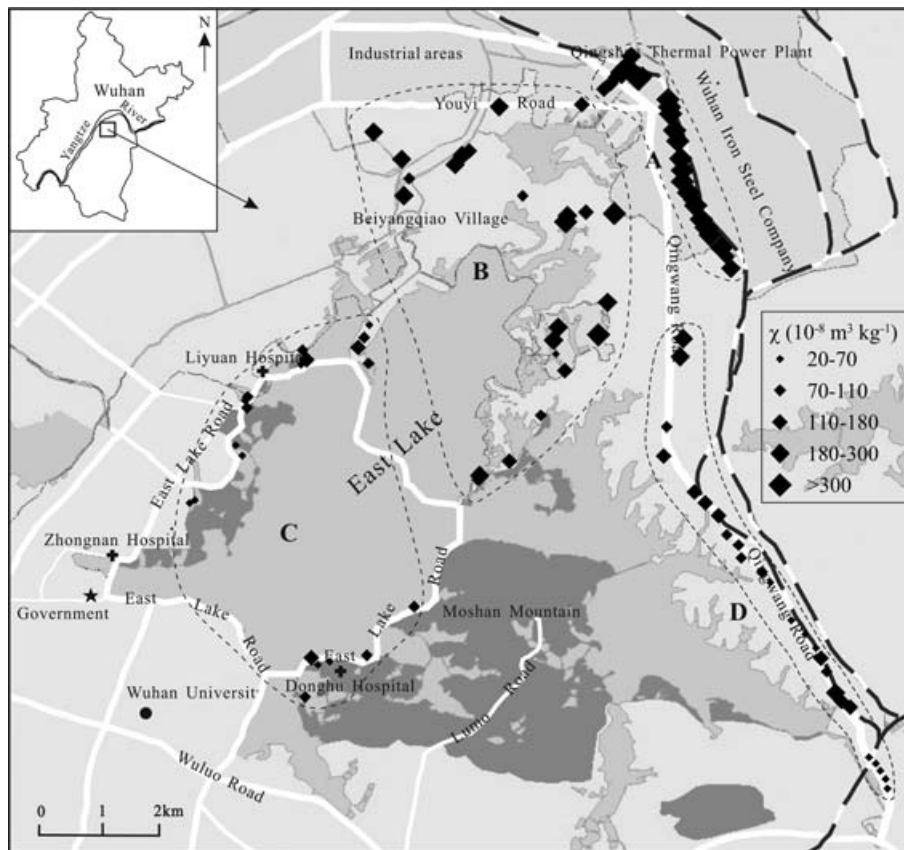


Figure 1. Location of the study areas with sampling points (rhombic symbols) and the distribution pattern of the topsoil magnetic susceptibility. A-WG area, B-BYQ area, C-ELR area and D-QWR area. The size of the rhombic symbols represents the magnitude of the magnetic susceptibility.

30 cm in BYQ and QWR areas. A total of 100 topsoil samples and 33 subsoil samples were obtained for this study.

2.3 Magnetic measurements

Magnetic measurements were completed in Geophysical Laboratory of The University of Hong Kong and Petrophysical Laboratory of China University of Geosciences (Wuhan). The low-field magnetic susceptibility (χ) was measured using an AGICO KLY-3S Kappabridge. Magnetic susceptibilities at dual frequencies (0.47 and 4.7 kHz) were measured using a Bartington MS2B dual-frequency sensor. The values are expressed as mass-normalized susceptibility χ_{lf} and χ_{hf} , respectively. Frequency dependent susceptibility was then calculated from the two values and expressed as a percentage χ_{fd} per cent = $(\chi_{lf} - \chi_{hf})/\chi_{lf} \times 100$ per cent.

Anhyseretic remanent magnetization (ARM) was imparted using a peak alternating field (AF) of 100 mT with a direct current (DC) bias field of 0.05 mT parallel to the AF, and measured using a Molspin magnetometer. Isothermal remanent magnetization (IRM) measurements were carried out by using ASC scientific model IM-10 impulse magnetizer and Molspin magnetometer. IRM acquired in a peak field of 1 T was regarded as saturation IRM (SIRM), whereas IRM acquired in a backdemagnetization field of 300 mT was named IRM_{-300mT}. IRM_{-300mT}/SIRM (*S*-ratio) was used to define approximately the relative concentration of the remanence-carrying ferro(i)magnetic minerals (Thompson & Oldfield 1986). In addition, a number of representative samples were magnetized in step-wise growing DC fields to obtain the IRM acquisition curves, 12 forward steps from 7 to 1100 mT were used.

High-temperature dependence of magnetic susceptibility was studied to determine Curie temperature (T_c) using MS2 κ/T system. Measurements were performed from room temperature up to

700 °C, and the measurement interval was 2 °C with heating and cooling rate of 5 °C min⁻¹ and 10 °C min⁻¹, respectively.

2.4 Heavy metal analyses

Concentrations of heavy metal for 49 representative samples were analysed. A small portion of the sample (approximately 1.0000 g) was digested in 12 ml of 68 per cent nitric acid. The digested solutions were diluted and filtered to 50 ml with deionized water for analyses. Concentrations of heavy metals, such as Co, Cr, Cu, Mn, Ni, Pb and Zn, etc. were determined using inductively coupled plasma atomic emission spectroscopy (ICP-AES). A blank sample was prepared in the same way and used as the background. Ten per cent of samples were measured repeatedly for the purpose of quality control. The analytical precision, measured by the relative standard deviation of parallel samples was less than 5 per cent.

3 RESULTS

3.1 Magnetic properties

3.1.1 Magnetic susceptibility

The magnetic parameters of the urban soils are summarized in Table 1 and the χ of topsoils are shown in Fig. 1. The χ of topsoils in WG and BYQ are generally higher than those in QWR and ELR (Fig. 1). The average χ values of topsoils from WG, BYQ, QWR and ELR are 539.92, 204.31, 105.89 and $82.68 \times 10^{-8} \text{ m}^3 \text{ kg}^{-1}$, respectively. The mean χ of topsoils in BYQ and QWR are about four and two times higher than that of the subsoils, respectively (Fig. 2). Because most of the samples are collected from the farmland, the large variation of χ of subsoil samples and the

Table 1. Magnetic parameters of the urban soils.

Magnetic parameters		WG (<i>n</i> = 25)	BYQ (<i>n</i> = 41)		QWR (<i>n</i> = 43)		ELR (<i>n</i> = 24)
			Topsoils (<i>n</i> = 25)	Subsoils (<i>n</i> = 16)	Topsoils (<i>n</i> = 26)	Subsoils (<i>n</i> = 17)	
χ ($10^{-8} \text{ m}^3 \text{ kg}^{-1}$)	Range	113.52–1383.79	55.78–583.85	16.32–123.36	28.80–293.49	5.76–148.46	11.91–164.40
	Mean \pm SD	539.92 \pm 354.28	204.31 \pm 112.84	52.12 \pm 30.88	105.89 \pm 72.37	56.20 \pm 46.34	82.68 \pm 42.74
χ_{fd} (per cent)	Range	0.6–3.8	0.4–5.5	0.5–9.5	0.5–6.1	0.7–10.1	1.5–5.8
	Mean \pm SD	1.7 \pm 1.03	2.5 \pm 1.54	4.5 \pm 2.42	2.9 \pm 1.77	4.9 \pm 3.20	3.5 \pm 1.31
ARM ($10^{-5} \text{ Am}^2 \text{ kg}^{-1}$)	Range	20.67–102.15	7.44–44.72	0.71–28.66	2.04–59.89	0.18–32.60	0.71–47.80
	Mean \pm SD	48.10 \pm 24.00	21.85 \pm 10.25	8.71 \pm 7.47	15.05 \pm 13.63	10.20 \pm 10.95	17.21 \pm 12.06
SIRM ($10^{-5} \text{ Am}^2 \text{ kg}^{-1}$)	Range	848.02–14851.41	334.98–5879.44	95.68–1206.99	287.53–4042.19	48.49–1136.96	143.24–2824.91
	Mean \pm SD	5665.19 \pm 3830.51	2384.46 \pm 1289.98	613.11 \pm 343.74	1233.48 \pm 1067.92	438.40 \pm 327.58	881.97 \pm 613.54
<i>S</i> -ratio	Range	0.81–0.96	0.83–0.94	0.61–0.91	0.79–0.94	0.56–0.91	0.63–0.91
	Mean \pm SD	0.89 \pm 0.03	0.894 \pm 0.03	0.81 \pm 0.08	0.86 \pm 0.04	0.78 \pm 0.11	0.85 \pm 0.06

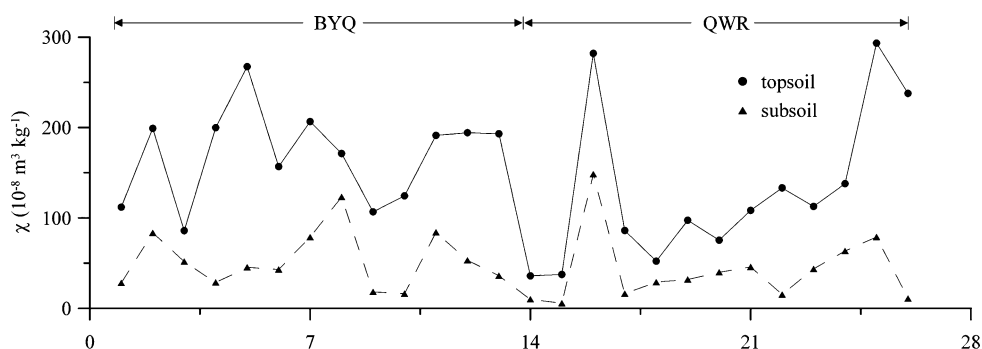


Figure 2. Comparison of magnetic susceptibility of topsoils and subsoils from BYQ and QWR.

small differences of χ between topsoil and subsoil (Fig. 2) are probably caused by physical migration and homogenization of magnetic particles during the plowing process (Magiera *et al.* 2006).

The mean values of χ_{fd} per cent of topsoils are 1.7 per cent in WG, 2.5 per cent in BYQ, 2.9 per cent in QWR and 3.5 per cent in ELR, respectively. The χ_{fd} per cent of subsoils ranges from 0.5 to 9.5 per cent with mean value of 4.5 per cent in BYQ, and from 0.7 to 10.1 per cent with mean value of 4.9 per cent in QWR, respectively (Table 1). This indicates that subsoils contain more superparamagnetic (SP) particles than topsoils (Dearing *et al.* 1996).

3.1.2 Remanent magnetization

ARM and SIRM of the topsoils peak at WG (Table 1). The mean ARM of topsoils is the lowest in QWR. The mean SIRM in ELR is much lower than that of the other three sites. In addition, the mean values of χ , ARM and SIRM show comparable decreasing trend from WG, to BYQ, to QWR and to ELR. This trend is opposite to that of the mean χ_{fd} per cent value (Table 1). If SP particles dominate the magnetic enhancement of the topsoils, we expect a positive correlation between χ and χ_{fd} per cent. Therefore, the negative correlation between these two parameters suggests that magnetic enhancement is due to the input of coarser-grained magnetic particles.

IRM acquisition curves for representative samples are shown in Fig. 3. Curves of topsoils rapidly reach saturation at magnetic field lower than 200 mT, whereas subsoils are usually saturated at magnetic field greater than 400 mT. This indicates that topsoil is dominated by strongly magnetic ferrimagnetic minerals. In contrast, significant amount of antiferromagnetic minerals (hematite and goethite) are present in the subsoils (Thompson & Oldfield 1986). This can be further confirmed by the lower mean S -ratios (0.78–0.81) for the subsoils (Table 1).

3.1.3 Temperature-dependent magnetic susceptibility ($\chi-T$)

The normalized $\chi-T$ curves of representative samples reveal different behaviours between topsoil and subsoil samples (Fig. 4). The heating run of topsoil samples (Fig. 4a) gradually increases to

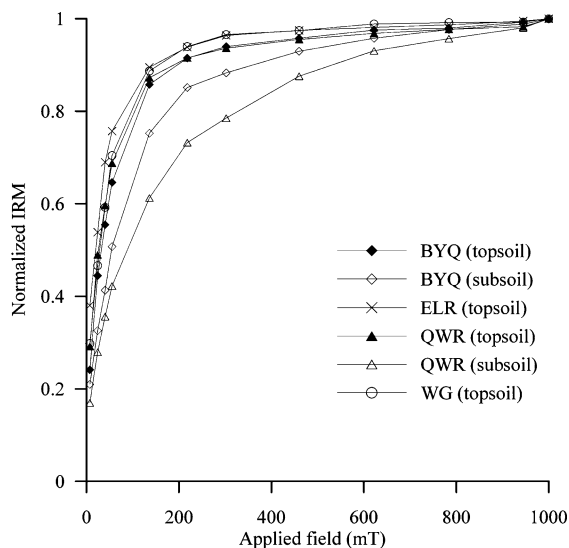


Figure 3. Isothermal remanent magnetization (IRM) acquisition curves for representative samples.

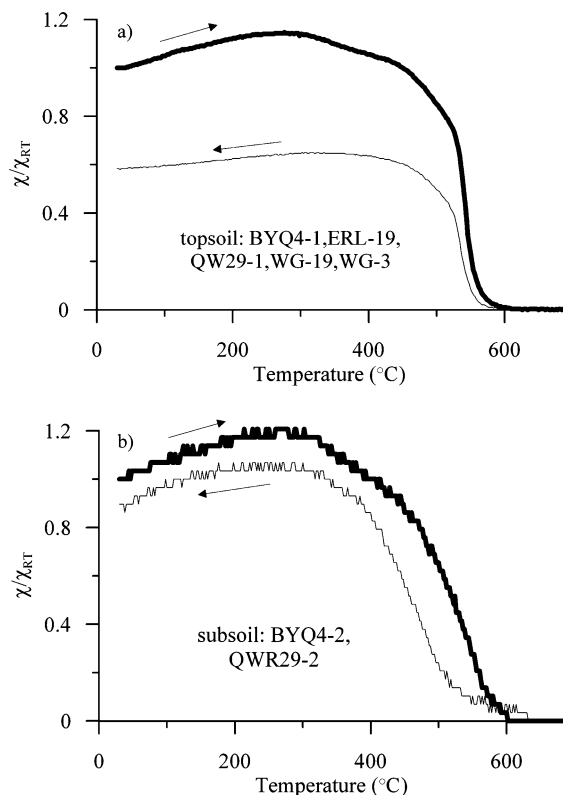


Figure 4. Curves of temperature-dependent magnetic susceptibility for representative topsoils samples (a) and subsoils samples (b). Each curve was normalized with its corresponding magnetic susceptibility at room temperature χ_{RT} . The thick and thin lines denote heating and cooling runs, respectively.

280 °C due to unblocking of single domain magnetic particles (Liu *et al.* 2005). Between 300 and 420 °C, the decrease in susceptibility is often related to the transformation of maghemite to hematite (Dunlop & Özdemir 1997; Kosterov 2002; Liu *et al.* 2005). The Curie temperature (T_c) of 580 °C indicates the presence of magnetite (Dunlop & Özdemir 1997). The cooling curve shows a significant decrease in susceptibility further confirms the transformation from maghemite to hematite.

The $\chi-T$ curves for the subsoils are almost reversible except for slight decrease in χ after the thermal treatment. χ peaks at about 300 °C for both heating and cooling curves and thus correspond to the unblocking temperature of single domain magnetic particles. The T_c of 580 °C for the heating curve indicates that the magnetic phase is magnetite. For the cooling curve, hematite appears as shown by the T_c of 640 °C. This is also consistent with the transformation of maghemite to hematite.

In summary, the $\chi-T$ curves reveal that the dominant ferrimagnetic minerals in both top- and subsoils are magnetite. Maghemite is also present probably due to the low-temperature oxidation of magnetite (Dunlop & Özdemir 1997). Moreover, the subsoils exhibit a lower unblocking temperature than the topsoils, which indicates that the magnetite particles in the subsoils are much finer than those in the topsoils.

3.2 Heavy metal concentrations

Concentrations of several heavy metals are given in Table 2. The concentrations of Cu, Pb, Zn and their corresponding background

Table 2. Heavy metal concentrations (unit: mg kg⁻¹) and PLI for urban soils.

		Topsoils (n = 38)				Subsoils (n = 11)	Background value ^a
		WG (n = 12)	BYQ (n = 9)	QWR (n = 8)	ELR (n = 9)		
Co	Range	22.44–33.13	21.37–28.33	17.17–30.41	12.57–26.57	22.64–29.76	15.4
	Mean ± SD	26.00 ± 3.65	23.91 ± 2.59	25.68 ± 4.43	20.58 ± 4.74	26.54 ± 2.15	
Cr	Range	59.23–93.76	57.36–95.16	42.15–85.82	37.44–76.30	51.25–78.76	86.0
	Mean ± SD	67.83 ± 9.77	68.90 ± 11.48	65.17 ± 13.58	58.60 ± 13.29	66.04 ± 8.82	
Cu	Range	45.12–129.70	43.98–95.08	37.24–60.68	23.09–72.75	28.95–58.33	30.7
	Mean ± SD	83.54 ± 30.78	62.78 ± 15.01	48.64 ± 8.46	44.16 ± 14.10	43.53 ± 9.37	
Pb	Range	28.93–95.70	26.97–57.11	30.46–57.24	16.29–44.33	20.84–31.93	26.7
	Mean ± SD	51.89 ± 19.71	34.03 ± 9.20	38.57 ± 8.69	25.32 ± 8.42	25.18 ± 4.00	
Zn	Range	132.40–381.20	97.36–182.40	111.50–244.30	54.25–169.90	69.98–142.6	83.6
	Mean ± SD	214.67 ± 75.24	130.12 ± 27.23	150.45 ± 49.76	96.09 ± 36.08	100.98 ± 22.92	
PLI	Range	1.32–2.42	1.15–1.96	1.18–1.83	0.66–1.61	0.93–1.43	
	Mean ± SD	1.69 ± 0.37	1.37 ± 0.23	1.38 ± 0.24	1.07 ± 0.29	1.16 ± 0.17	

^aAfter China Environmental Monitoring Station (1990).

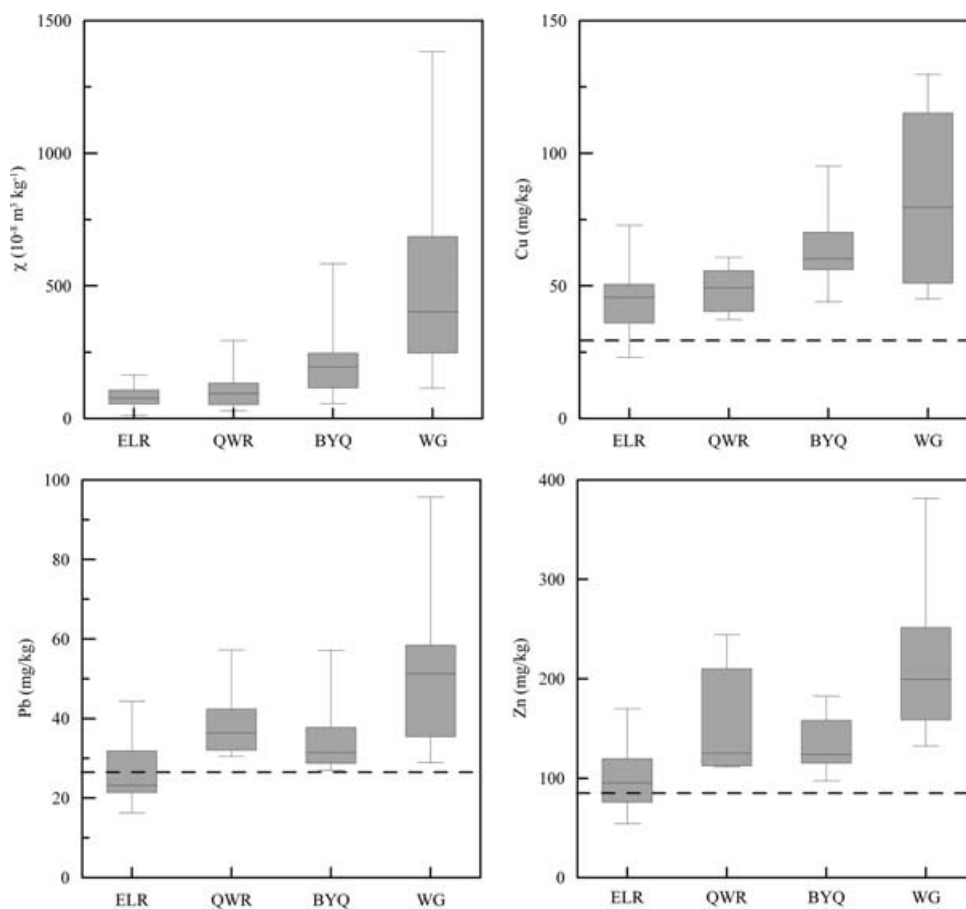


Figure 5. Box-plots of magnetic susceptibility, concentration of Cu, Pb and Zn in urban topsoils. The dash lines mark the background values of heavy metal concentration of soils in Wuhan, China (China Environmental Monitoring Station 1990).

values in Wuhan (China Environmental Monitoring Station 1990) are compared in Fig. 5. The mean concentrations of Co and Cr are comparable both in topsoils and subsoils in four areas. The concentrations of Cu, Pb and Zn in topsoils in WG, BYQ and QWR are up to four times higher than their corresponding background values, and obviously higher than these of subsoils. Mean concentrations of Cu, Pb and Zn in topsoils from WG and BYQ are much higher than those from ELR (Table 2).

Furthermore, we used the Tomlinson pollution load index (PLI) (Angulo 1996) to assess the relative heavy metal toxicity of the soils and how much a sample exceeds the concentrations of heavy metals for natural environments. The PLI index is defined as the n th root of the multiplication of the concentration factors (CF_{HM}), where CF_{HM} is the ratio between the concentration of each heavy metal (C_{HM}) to its corresponding background value ($C_{background}$) or the lowest concentration values detected for each heavy

Table 3. Correlation coefficients between heavy metals concentration and magnetic parameters in urban soils ($n = 49$).

	Co	Cr	Cu	Pb	Zn	PLI
χ	0.111	0.017	0.736 ^a	0.675 ^a	0.678 ^a	0.631 ^a
ARM	0.051	0.049	0.612 ^a	0.563 ^a	0.620 ^a	0.544 ^a
SIRM	0.117	0.058	0.792 ^a	0.727 ^a	0.720 ^a	0.684 ^a
IRM _{-300mT}	0.110	0.056	0.791 ^a	0.723 ^a	0.714 ^a	0.680 ^a

^aCorrelation is significant at the 0.01 level (two-tailed).

metal,

$$CF_{HM} = C_{HM}/C_{background}, \quad (1)$$

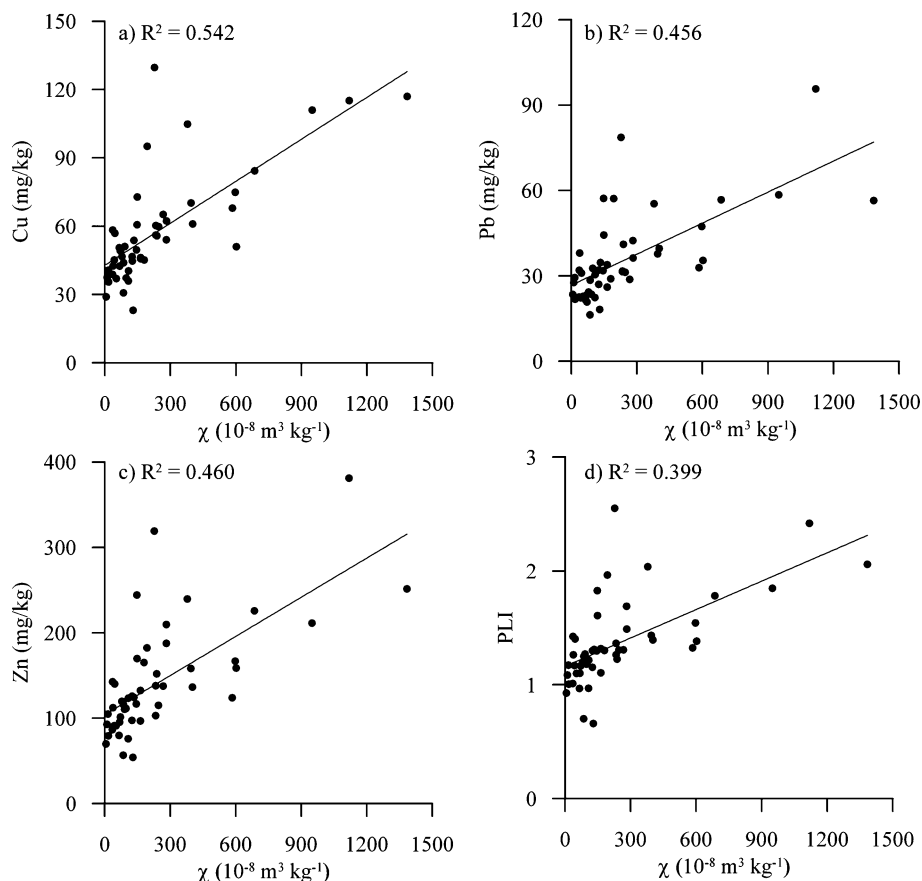
and

$$PLI = \sqrt[n]{CF_{HM1} \times CF_{HM2} \times \dots \times CF_{HMn}}. \quad (2)$$

Table 2 shows that the mean PLI of the topsoils in WG is the highest (up to 1.69), but the lowest in ELR (Table 2).

3.3 Correlations between magnetic parameters and heavy metals concentrations

Table 3 lists the Pearson's correlation coefficients between the concentration of heavy metals and magnetic parameters. The correlation matrix indicates that χ , ARM, SIRM and IRM_{-300mT} all have a strong linear correlation with heavy metal concentrations except for Co and Cr (Table 3). Significant correlations between χ , heavy metal concentrations, and PLI can be clearly seen from the scatter plots shown in Fig. 6. Similar close correlation were also found in the sediments of the East Lake (Liu *et al.* 2006)

**Figure 6.** Scatter plots of mass-specific susceptibility versus concentration of Cu, Pb, Zn and PLI.

4 DISCUSSIONS

4.1 Magnetic carriers and grain sizes

The χ - T (Fig. 4) and the IRM acquisition curves (Fig. 3) reveal that magnetite is the dominant ferromagnetic phase in both top- and subsoils. Maghemite is also present in both groups but more significant in the topsoils. This indicates that the maghemite is more related to the coarse-grained magnetite in the topsoils, most probably due to the low-temperature oxidation of magnetite. Antiferromagnetic minerals (hematite and goethite) also present in the samples evident by the low S -ratios. However, for the other magnetic proxies, especially for χ , ARM and SIRM, hematite signals have been masked by the magnetite signals.

χ_{fd} per cent is sensitive to the SP component. If χ_{fd} per cent > 4 per cent, the assemblage of magnetic grains contains a significant portion of SP particles; in the case of χ_{fd} per cent < 4 per cent, the portion of SP particles is low (Dearing *et al.* 1996; Petrovský *et al.* 2000a). Accordingly, magnetic carriers in the topsoils from WG (with mean χ_{fd} per cent of 1.7 per cent) are predominately coarser grains; for topsoils from BYQ, QWR and ELR (with mean χ_{fd} per cent of 2.5, 2.9 and 3.5 per cent, respectively), it appears possibly an admixture of a small amount of SP grains with coarse grains; there are much more SP grains in the subsoils (with mean χ_{fd} per cent of 4.5 and 4.9 per cent in BYQ and QWR, respectively). King *et al.* (1982) proposed a dimensionless ratio between anhysteretic susceptibility and low-field susceptibility (κ_{ARM}/κ_{lf}) to provide some constraints on grain size of ferro(i)magnets in samples. As King plot shown in Fig. 7(a), there is a clear tendency of occurrence of coarser

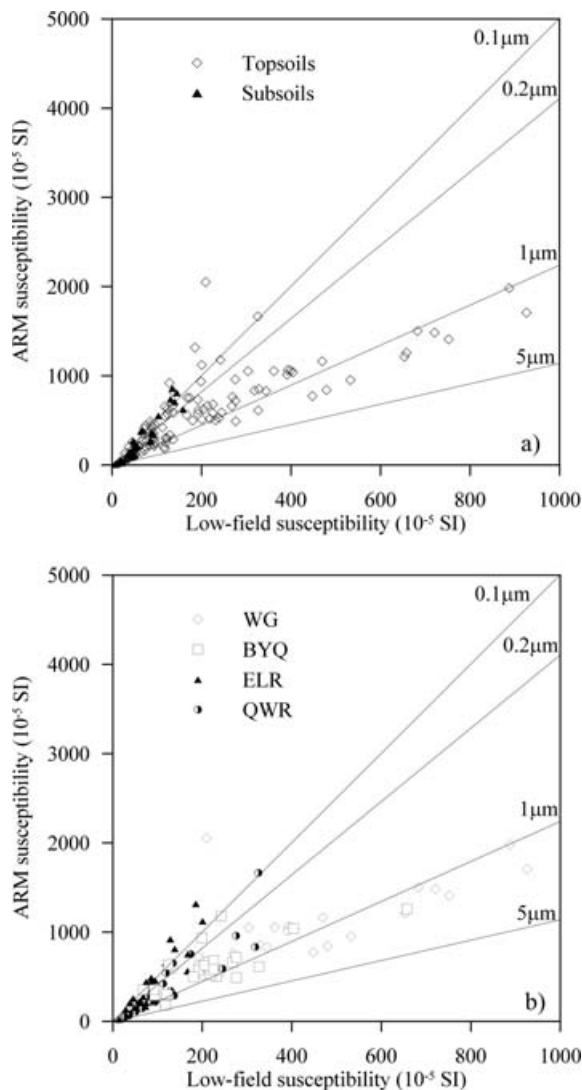


Figure 7. Anhysteretic susceptibility (κ_{ARM}) versus low-field susceptibility (κ_{LF}) for (a) all samples and (b) topsoil samples. The grain size has been estimated from the calibration straight (King *et al.* 1982).

grains (0.2–5.0 μm) and also higher magnetic concentration in topsoils. However, the subsoils are mainly in a different range of 0.1 ~ 0.5 μm . In addition, a highly significant correlation ($r = 0.979$) between χ and $\text{IRM}_{-100\text{mT}}$ for the topsoils suggests that the magnetic susceptibility of urban topsoils is predominately controlled by coarse-grained ferrimagnetic minerals.

ARM/SIRM is also widely employed as an indicator for magnetic grain size in a sample. High concentrations of small particles yield higher values because they are more efficient at acquiring remanence, in particular ARM (Maher 1988; Dunlop 1995). As shown in Fig. 8, the topsoil samples are clustered into two different groups: the slope of ARM of the topsoils from ELR and QWR is steeper, and yield higher ARM/SIRM ratios, suggesting that these samples containing a higher fraction of small (e.g. single domain, SD) particles. In contrast, the increases in SIRM and decreases in ARM/SIRM reflect an increase in both total magnetic mineral concentrations and the relative importance of coarser (PSD/MD) magnetic particles in topsoils from WG and BYQ (Thompson & Oldfield 1986; Maher 1988). It could also be confirmed by King plot (Fig. 7b), the es-

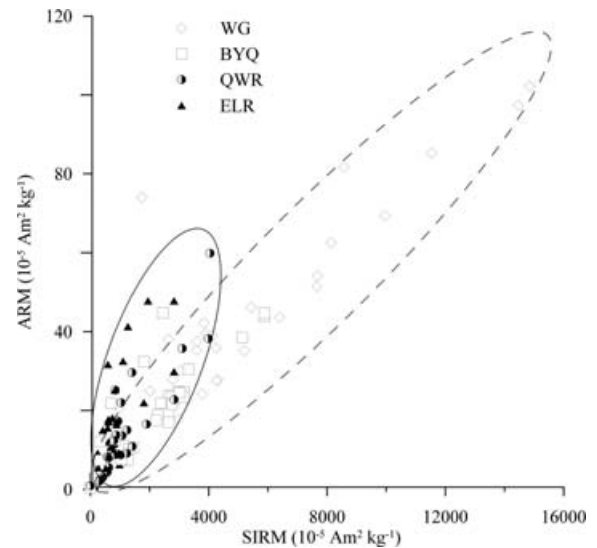


Figure 8. Scatter plot of anhysteretic remanent magnetization (ARM) versus saturation isothermal remanent magnetization (SIRM) of all topsoils.

timated grain size of magnetic particles in topsoils from WG and BYQ are mainly located in ~1 μm whereas that from ELR and QWR smaller than 0.5 μm .

In summary, the subsoils contain finer magnetite grains in SP + SD grain size region. In contrast, the topsoils contain more coarser-grained magnetite particles mostly in PSD or MD grain size region, and the magnetic particles in topsoils from WG and BYQ are coarser than those from QWR and ELR.

4.2 Sources of magnetic particles and heavy metals

Magnetic minerals in urban soils may be either inherited from the parent rocks (lithogenic origin), formed during pedogenesis and/or may stem from anthropogenic activities (secondary ferro (i) magnetic materials) (Boyko *et al.* 2004; Hanesch & Scholger 2005). The lithogenic influence on the topsoil magnetic susceptibility can be excluded by the significant enhancement of the topsoil susceptibility (Fialova *et al.* 2006; Magiera *et al.* 2006), which is about four and two times higher than that of the subsoil in BYQ and QWR (Table 1, Fig. 2). Together with the high values of χ , SIRM, S -ratio, low χ_{fd} per cent, and coarse-grained (PSD/MD) magnetite as the primary magnetic carrier, it reveals that the magnetic properties of the topsoils are major controlled by ferrimagnetic minerals with anthropogenic origin (Strzyszc & Magiera 2001; Fialova *et al.* 2006; Magiera *et al.* 2006).

Specifically, the emission and windblown fly ashes from WISG and QTPP should be responsible for the high concentration of magnetic minerals and elevated concentration of heavy metals in the topsoils in WG and BYQ areas. In WG area, the mean value of χ is as high as $539.92 \times 10^{-8} \text{ m}^3 \text{ kg}^{-1}$, and the mean concentrations of Cu, Pb and Zn are, respectively, 2.7, 1.9 and 2.6 times higher than their corresponding background values (Table 2). Magnetic particles are formed both during the high temperature combustion of fossil fuels used for power generation and the process of metallurgical and smelting industry (Hullet *et al.* 1980; McLennan *et al.* 2000; Veneva *et al.* 2004). During fly ash formation, heavy metals are adsorbed on the surface of iron oxides (mainly magnetite) in a

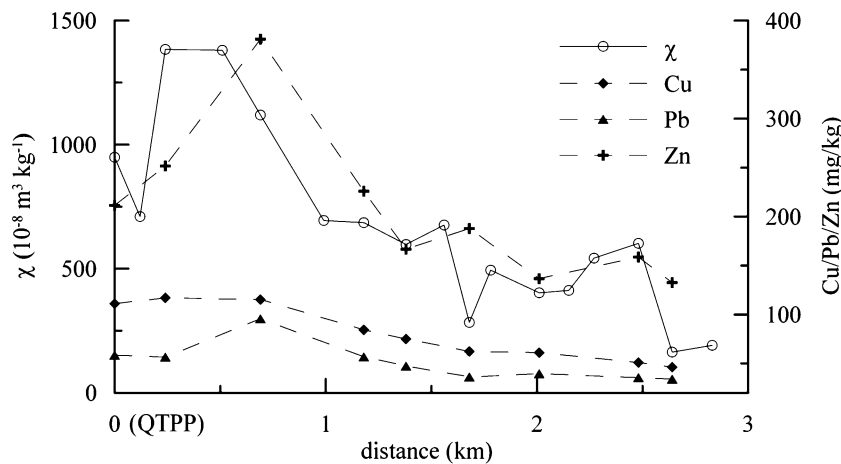


Figure 9. Comparison of magnetic susceptibility and the heavy metals concentration in the topsoils at different distances far from Qingshan Thermal Power Plant (QTPP, located in '0' point) in WG area.

preferential order of Pb, Zn, Cu, Cr, Cd (Georgeaud *et al.* 1997) or substituted spinels of $\text{Fe}_{3-x}\text{M}_x\text{O}_4$ (Hansen *et al.* 1981; Hunt *et al.* 1984), also the central background of the potential link between heavy metals and magnetic particles could be the 'same source-same distribution pathway' principle (Spiteri *et al.* 2005). Nevertheless, the deposition of these magnetic particles on the soils surface made a significant contribution to the magnetic component and heavy metals concentrations in topsoils, especially in industrial areas (e.g. WG area) and downwind regions (e.g. BYQ area) (Strzyszczyk & Magiera 1998; Gołuchowska 2001). Flanders (1994) suggested that the fossil fuel burning produce magnetite with an estimated concentration of 50–10 000 ppm are potentially the most significant source of anthropogenic ferrimagnetics in the upper soil. A great deal of coarse-grained Fe-rich spherules with industrial origin were found in topsoils layer in Bulgaria by Veneva *et al.* (2004), in the Lausitz area, Eastern Germany by Spiteri *et al.* (2005) and in Czech Republic by Fialova *et al.* (2006). Generally, the amount of settled magnetic particles and heavy metals in the topsoils decreases with increasing distance far from the emission source (Hoffmann *et al.* 1999; Kapička *et al.* 1999), this tendency is also found in WG area (Fig. 9).

Although the prevailing wind direction is NE, it is occasional and the wind speed is relatively weak. Therefore, it can be assumed that long distance transported particles originated from WISG and QTPP are less significant than local pollution sources (e.g. vehicle traffics) in the ELR area. Consequently, the elevated concentrations of heavy metals and magnetic particles in topsoils from ELR and QWR should be predominately attributed to vehicle traffics. The exhaust emissions and abrasion/corrosion of engine and/or vehicle body material often contain a great deal of magnetite-like particles agglomerated with Cu, Pb and Zn (Hopke *et al.* 1980; Kim *et al.* 1998; Hoffmann *et al.* 1999; Petrovský *et al.* 2000b; Kapička *et al.* 2003). Lu *et al.* (2005) found that the average concentrations of Cu, Cd, Pb and Fe in automobile emission particulates were, respectively, 95.83, 22.14, 30.58 and 34727.31 mg kg^{-1} in Hangzhou, China. However, the vehicles travelling on the East Lake Road located in East Lake Scenic Area are mainly buses, taxies and cars, and many trees are growing on the roadsides. On the contrary, Qingwang Road has relatively heavy traffic loads. Besides buses and taxies, a great deal of trucks transporting different materials (e.g. raw materials and produces of the WISG) were driven on this road. This may have resulted in the higher enhancement of magnetic particles

and heavy metal concentrations in topsoils in QWR than those in ELR.

The magnetism and the concentrations of Cu, Pb and Zn in topsoils from WG, BYQ is much higher than those from QWR and ELR (Fig. 1, Tables 1 and 2), and the grain size of magnetic particles in the first two areas are significantly coarser than those in the latter areas (Figs 7b and 8). These differences are indicative of the differences in sources of magnetic particles. Vehicles have been suggested to generally produce non-spherical magnetite particles via exhaust emissions and the abrasion or corrosion of the vehicle engine and body work (Matzka & Maher 1999), with the majority of particles smaller than 2.5 μm in diameter (Silva & Prather 1997). Following the granulometric analysis, most of the magnetic fraction in coal-fired fly ash is present in the grain size fraction from 2 to 50 μm (Strzyszczyk *et al.* 1996), even up to ~500 μm (Sokol *et al.* 2000). Furthermore, vehicular emissions are dominated principally by ferrimagnetic particles whereas magnetically harder behaviour is observed for fly ash samples, because of the presence of hematite (Lecoanet *et al.* 2003). These differences in magnetic grain size and minerals make it is possible to discriminate the sources between fly ash from power stations and particulate emissions of vehicles using magnetic methods (Hunt *et al.* 1984; Lecoanet *et al.* 2003).

4.3 Magnetic parameters as indicators of heavy metals contamination in urban soils

Generally, magnetic measurements as a tool for evaluating pollutions are based on two reasons. First, the magnetic parameters (e.g. magnetic susceptibility) of soils are greater than its corresponding background. Secondly, magnetic parameters have significant correlations with the concentrations of pollutants (Versteeg *et al.* 1995). In the present study, the magnetic susceptibility of topsoils is much higher than that of the subsoils, the differences between them range from 23.12 to $226.86 \times 10^{-8} \text{ m}^3 \text{ kg}^{-1}$ with an average of $102.63 \times 10^{-8} \text{ m}^3 \text{ kg}^{-1}$ (Table 1, Fig. 2). In addition, the magnetic susceptibility of topsoils significantly correlates with Cu, Pb, Zn and PLI, their Pearson's correlation coefficients are 0.736, 0.675, 0.678 and 0.631, respectively (Table 3, Fig. 6). These results propose that magnetic susceptibility can actually serve as an effective indicator for mapping the heavy metal pollutions in the East Lake region, Wuhan, China.

5 CONCLUSIONS

In this paper, detailed magnetic measurements and heavy metal analyses were performed on 133 urban soil samples from four areas with different environmental setting around the East Lake in Wuhan, China. Magnetism and concentrations of heavy metals of topsoils are significantly elevated. For instance, the average magnetic susceptibility, the mean concentrations of Cu, Pb and Zn for topsoils in WG (a heavy industrial area hosting thermal power plant and steel works) peak in the study areas, followed by BYQ (downwind villages of WG), QWR (a main-road with heavy traffic), and ELR (roads around the East Lake, a famous scenic spot). The predominant magnetic carrier in urban topsoils is PSD/MD magnetite. The elevated magnetism and heavy metal concentration are attributed to anthropogenic and industrial activities. However, the sources of magnetic particles and heavy metals are different to a certain extent, such as the emission and windblown fly ashes from the WISG and QTPP should be the predominant sources of magnetic particles and heavy metals in topsoils from WG and BYQ; the exhaust emissions and abrasion and corrosion of engine and vehicle body material resulted in the enhancements of magnetism and heavy metals concentration in the topsoils from QWR and ELR at different degree, respectively. Concentration-related magnetic parameters, for example, magnetic susceptibility, ARM, SIRM and IRM_{-300mT} all have significant linear correlation with the concentration of Cu, Pb, Zn and PLI. However, the grain sizes of the magnetic particles of different origins differ greatly. For example, the magnetic particles in topsoils from WG and BYQ are coarser than that in topsoils from QWR and ELR. Therefore, it is possible to discriminate the different sources of magnetic particulate using magnetic methods, and then further link to the pollution sources in urban settings.

ACKNOWLEDGMENTS

This study was supported by the National Natural Science Foundation of China (No. 40474025). We thank Dr Shouyun Hu for his generous help and fruitful discussions, and two anonymous reviewers for their valuable comments on the manuscript. We are also grateful to Dr Yaoguo Li and Qingsong Liu for their useful discussions and English improvement of the manuscript.

REFERENCES

- Angulo, E., 1996. The Tomlinson pollution load index applied to heavy metal "Mussel-Watch" data: a useful index to assess coastal pollution, *Sci. Tot. Environ.*, **187**, 19–56.
- Boyko, T., Scholger, R., Stanjek, H. & MAGPROX Team, 2004. Topsoils magnetic susceptibility mapping as a tool for pollution monitoring: repeatability of in situ measurements, *J. Appl. Geophys.*, **55**, 249–259.
- China Environmental Monitoring Station, 1990. *Background Values of Elements in Soils of China*, China Environmental Press, Beijing (in Chinese).
- Dearing, J.A., Hay, K.L., Baban, S.M.J., Huddleston, A.S., Wellington, E.M.H. & Loveland, P.J., 1996. Magnetic susceptibility of soil: an evaluation of conflicting theories using a national data set, *Geophys. J. Int.*, **127**, 728–734.
- Dearing, J.A., Hannam, J.A., Anderson, A.S. & Wellington, E.M.H., 2001. Magnetic, geochemical and DNA properties of highlymagnetic soils in England, *Geophys. J. Int.*, **144**, 183–196.
- DeKimpe, C.R. & Morel, J.L., 2000. Urban soil management: a growing concern, *Soil Sci.*, **165**(1), 31–40.
- Dunlop, D.J. & Özdemir, Ö., 1997. *Rock Magnetism: Fundamentals and Frontiers*, Cambridge University Press, Cambridge.
- Dunlop, D.J., 1995. Magnetism in rocks, *J. geophys. Res.*, **100**, 2161–2174.
- Fialova, H., Maier, G., Petrovský, E., Kapička, A., Boyko, T., Scholger, R. & MAGPROX Team, 2006. Magnetic properties of soils from sites with different geological and environmental settings, *J. Appl. Geophys.*, **59**, 273–283.
- Flanders, P., 1994. Collection, measurement, and analysis of airborne magnetic particles from pollution in the environment, *Appl. Phys.*, **75**, 5931–5936.
- Georgeaud, V.M., Rochette, P., Ambrosi, J.P. & Bottero, J.Y., 1997. Heavy metal sorption and magnetic properties of magnetite: a case study, in *Book of Abstracts, 8th Scientific Assembly of IAGA*, 4–14 August 1997, Uppsala, Sweden.
- Gołuchowska, B.J., 2001. Some factors affecting an increase in magnetic susceptibility of cement dusts, *J. Appl. Geophys.*, **48**, 103–112.
- Hanesch, M. & Scholger, R., 2005. The influence of soil type on the magnetic susceptibility measured throughout profiles, *Geophys. J. Int.*, **161**, 50–56.
- Hansen, L.D., Silbermann, D. & Fisher, G.L., 1981. Crystalline components of stack-collected, size-fractionated coal fly ash, *Environ. Sci. Technol.*, **15**, 1057–1062.
- Heller, F., Strzyszcza, Z. & Magiera, T., 1998. Magnetic record of industrial pollution in forest soils of Upper Silesia, Poland, *J. geophys. Res.*, **103**, 17 767–17 774.
- Hoffmann, V., Knab, M. & Appel, E., 1999. Magnetic susceptibility mapping of roadside pollution, *J. Geochem. Explor.*, **66**, 313–326.
- Hopke, P.K., Lamb, E.R. & Natusch, D.F.S., 1980. Multielemental characterization of urban roadway dust, *Environ. Sci. Technol.*, **14**, 164–172.
- Hullet, L.D., Weisberger, A.J., Northcutt, K.J. & Ferguson, M., 1980. Chemical species in fly ash from coal-burning power plants, *Science*, **210**, 1356–1358.
- Hunt, A., Jones, J. & Oldfield, F., 1984. Magnetic measurements and heavy metals in atmospheric particulates of anthropogenic origin, *Sci. Total Environ.*, **33**, 129–139.
- Jordanova, N.V., Jordanova, D.V., Veneva, L., Yorova, K. & Petrovský, E., 2003. Magnetic response of soils and vegetation to heavy metal pollution—A case study, *Environ. Sci. Technol.*, **37**, 4417–4424.
- Kapička, A., Jordanova, N., Petrovský, E. & Podrazský, V., 2003. Magnetic study of weakly contaminated forest soils, *Water Air Soil Pollut.*, **148**, 31–44.
- Kapička, A., Petrovský, E., Ustjak, S. & Machackova, K., 1999. Proxy mapping of fly ash pollution of soils around a coal-burning power plant: a case study in the Czech Republic, *J. Geochem. Explor.*, **66**, 291–297.
- Kim, K.W., Myung, J.H., Ahn, J.S. & Chon, H.T., 1998. Heavy metal contamination in dusts and stream sediments in the Taejon Area, Korea, *J. Geochem. Explor.*, **64**, 409–419.
- King, J., Banerjee, S.K., Marvin, J. & Özdemir, Ö., 1982. A comparison of different magnetic methods for determining the relative grain size of magnetite in natural materials: some results from lake sediments, *Earth Planet. Sci. Lett.*, **59**, 404–419.
- Kosterov, A., 2002. Low-temperature magnetic hysteresis properties of partially oxidized magnetite, *Geophys. J. Int.*, **149**, 796–804.
- Lecoanet, H., Lèveque, F. & Ambrosi, J.P., 2003. Combination of magnetic parameters: an efficient way to discriminate soil-contamination sources (south France), *Environ. Pollut.*, **122**, 229–234.
- Lecoanet, H., Lèveque, F. & Segura, S., 1999. Magnetic susceptibility in environmental applications: comparison of field probes, *Phys. Earth Planet. Inter.*, **115**, 191–204.
- Liu, Q.S., Deng, C.L., Yu, Y.J., Torrent, J., Banerjee, S.K. & Zhu, R.X., 2005. Temperature dependence of magnetic susceptibility in an argon environment: implications for pedogenesis of Chinese loess/paleosols, *Geophys. J. Int.*, **161**, 102–112.
- Liu, Z.D., Liu, Q.S., Wang, H.S., Wang, Z.Y., Yang, T. & Cao, G.D., 2006. Relationship between magnetic properties and heavy metals of sediments in Donhu Lake, Wuhan, China, *Earth Sci.—J. China Univ. Geosci.*, **31**(2), 266–272 (in Chinese with English abstract).
- Lu, S.G. & Bai, S.Q., 2006. Study on the correlation of magnetic properties and heavy metals content in urban soils of Hangzhou City, China, *J. Appl. Geophys.*, **60**, 1–12.

- Lu, S.G., Bai, S.Q., Cai, J.B. & Xu, C., 2005. Magnetic properties and heavy metal contents of automobile emission particulates, *J. Zhejiang Univ. SCI.*, **6B**(8), 731–735.
- Magiera, T., Strzyszczyk, Z., Kapička, A., Petrovský, E. & MAGPROX TEAM, 2006. Discrimination of lithogenic and anthropogenic influences on topsoil magnetic susceptibility in Central Europe, *Geoderma*, **130**, 299–311.
- Maher, B.A., 1988. Magnetic properties of some synthetic sub-micron magnetites, *Geophys. J.*, **94**, 83–96.
- Matzka, J. & Maher, B.A., 1999. Magnetic biomonitoring of roadside tree leaves: identification of spatial and temporal variations in vehicle-derived particulates. *Atmos. Environ.*, **33**, 4565–4569.
- McLennan, A.R., Bryant, G.W., Stanmore, B.R. & Wall, T.F., 2000. Ash formation mechanism during combustion in reducing conditions, *Energy Fuels*, **14**, 150–159.
- Petrovský, E., Alcalá, M.D., Criado, J.M., Grygar, T., Kapička, A. & Subrt, J., 2000a. Magnetic properties of magnetite prepared by ball-milling of hematite with iron, *J. Magn. Magn. Mater.*, **210**, 257–273.
- Petrovský, E., Kapička, A., Jordanova, N., Knab, M. & Hoffman, V., 2000b. Low-field magnetic susceptibility: a proxy method of estimating increased pollution of different environment systems, *Environ. Geol.*, **39**, 312–318.
- Schmidt, A., Yarnold, R., Hill, M. & Ashmore, M., 2005. Magnetic susceptibility as proxy for heavy metal pollution: a site study, *J. Geochem. Explor.*, **85**, 109–117.
- Shen, M.J., Hu, S.Y., Blaha, U., Yan, H.T., Rösler, W., Appel, E. & Hoffmann, V., 2006. Magnetic responses to heavy metal pollution and its statistics significance for site 722 soil vertical profile in Eastern Beijing, *Earth Sci.—J. China Univ. Geosci.*, **31**(3), 399–404 (in Chinese with English abstract).
- Silva, P.J. & Prather, K.A., 1997. On-line characterization of individual particles from automobile emissions, *Environ. Sci. Technol.*, **31**, 3074–3080.
- Sokol, E.V., Maksimova, N.V., Volkova, N., Nigmatulina, E. & Frenkel, A., 2000. Hollow silicate microspheres from fly ashes of the Chelyabinsk brown coals (South Urals, Russia), *Fuel Proc. Technol.*, **67**, 35–52.
- Spiteri, C., Kalinski, V., Rosler, W., Hoffmann, V., Appel, E. & MAGPROX team, 2005. Magnetic screening of a pollution hotspot in the Lausitz area, Eastern Germany: correlation analysis between magnetic proxies and heavy metal contamination in soils, *Environ. Geol.*, **49**, 1–9.
- Strzyszczyk, Z. & Magiera, T., 1998. Magnetic susceptibility and heavy metals contamination in soils of southern Poland, *Phys. Chem. Earth*, **23**, 1127–1131.
- Strzyszczyk, Z. & Magiera, T., 2001. Record of industrial pollution in Polish ombrotrophic peat bogs, *Phys. Chem. Earth (A)*, **26**, 859–866.
- Strzyszczyk, Z., Magiera, T. & Heller, F., 1996. The influence of industrial emissions on the magnetic susceptibility of soils in Upper Silesia, *Stud. Geoph. Geod.*, **40**, 276–286.
- Thompson, R. & Oldfield, F., 1986. *Environmental Magnetism*. Allen & Unwin, London.
- Veneva, L., Hoffmann, V., Jordanova, D., Jordanova, N. & Fehr, Th., 2004. Rock magnetic, mineralogical and microstructural characterization of fly ashes from Bulgarian power plants and the nearby anthropogenic soils, *Phys. Chem. Earth*, **29**, 1011–1023.
- Versteeg, J.K., Morris, W.A. & Rukavina, N.A., 1995. The utility of magnetic properties as a proxy for mapping contamination in Hamilton Harbor sediments, *J. Great Lakes Res.*, **21**, 71–83.
- Wang, X.S. & Qin, Y., 2006. Magnetic properties of urban topsoils and correlation with heavy metals: a case study from the city of Xuzhou, China, *Environ. Geol.*, **49**, 897–904.
- Yan, H.T., Hu, S.Y., Appel, E., Hoffmann, V. & Zhu, Y.X., 2005. Magnetic responses to vertical migration of fly ash in a soil profile, *Chin. J. Geophys.*, **48**, 1392–1399 (in Chinese with English abstract).